IIETA International Information and Engineering Technology Association
Advancing the World of Information and Engineering

Annales de Chimie - Science des Matériaux
Vol. 50, No. 2, April, 2026, pp. 149-156
Journal homepage: http://iieta.org/journals/acsm

# Effect of the Temperature on the Bio-Tribocorrosion Mechanisms for Ti-13Zr-13Nb in Artificial Saliva Solution

Fatima Ali Jaber*, Zuheir Talib Khulief

Metallurgical Engineering, Materials Engineering College, University of Babylon, Babylon 51001, Iraq

Corresponding Author Email: mat831.fatema.ali@student.uobabylon.edu.iq



https://doi.org/10.18280/acsm.500205

**Received:** 16 February 2026
**Revised:** 17 April 2026
**Accepted:** 25 April 2026
**Available online:** 30 April 2026

***Keywords:***
*tribocorrosion, temperature effect, dental implants, Ti13Zr13Nb alloy, electrochemical noise technique*

**ABSTRACT**

This work investigates the effect of temperature on the tribocorrosion behavior of a dental implant made of Ti-13Nb-13Zr alloy in artificial saliva simulating the oral environment. Reciprocating tribocorrosion tests were conducted using open circuit potential (OCP) measurements and the electrochemical noise (EN) technique at three temperatures (5, 37, and 60 ℃), with analysis of the mechanical and chemical contributions to the total volume loss. The results showed that temperature clearly affects the alloy behavior, On the other hand, the 60 ℃ condition had the least overall volume loss but the largest relative chemical contribution. This was attributed to the formation of a thickened, viscous oxide film acting as a 'protective cushion' that effectively shielded the metal substrate from direct mechanical abrasion. At 37 ℃, the alloy found the optimum balance between mechanical wear and repassivation, which shows the highest tribo-chemical stability in the body. At 5 ℃, the alloy lost the most total volume, where the mechanical contribution dominated due to temperature-induced brittleness and micro-cracking of the passive layer. The results, reported as mean ± SD, revealed a significant variation in total volume loss, with a 29.81% increase recorded at 5 ℃ and a sharp reduction of 71.00% at 60 ℃ compared to physiological conditions.

## 1. INTRODUCTION

Metals and their alloys are widely used as biomaterials. Titanium and its alloys are the most used, as they better meet the requirements of implant materials due to their superior properties such as low Young's modulus, excellent biocompatibility, and high corrosion resistance [1].

Dental implants, particularly those made of titanium, have become the most effective method for replacing missing teeth due to their high ability to achieve osseointegration [2]. Although commercially pure titanium (CP-Ti) is used in dental applications [1], its mechanical properties remain limited for applications requiring high wear resistance and high mechanical strength [3, 4]. At the same time, some first-generation alloys, such as Ti-6Al-4V, have shown toxic effects during long-term use, despite being the most widely used alloy in biomedical applications [5]. Studies have also indicated that these elements may hinder the osseointegration process after implantation [3, 4].

To address these concerns, attention has shifted toward second-generation titanium alloys, particularly β-phase alloys containing non-toxic elements such as zirconium (Zr) and niobium (Nb), which have been widely studied in biomedical applications [6, 7]. Studies have shown that β-modified titanium alloys possess superior properties for biomedical applications due to their lower elastic modulus. As a result, these vanadium-free alloys have become a focus of increasing research interest, and there is growing attention toward studying the response of these alloys to the tribocorrosion phenomenon [8].

Tribocorrosion is defined as a degradation process resulting from the synergistic interaction between mechanical effects and chemical or electrochemical corrosion on material surfaces. This phenomenon is more pronounced in environments where friction occurs simultaneously with corrosive agents, such as biological fluids or moisture, leading to a reduction in the service life of the material. In bone implants, tribocorrosion occurs due to continuous friction with bone in addition to the effect of biological fluids, leading to degradation of the implant surface [9, 10].

Previous studies have indicated that despite the extensive research on the properties of titanium, tribocorrosion behavior remains insufficiently investigated [11]. The limited research on the tribocorrosion behavior of a wide range of titanium alloys has led to ambiguity in determining the optimal composition of these alloys. Moreover, knowledge regarding the optimal microstructure remains insufficient, and the synergistic effect between corrosion and wear is often evaluated separately [5, 12]. Although interest in second-generation alloys for dental implant applications is increasing, information regarding the tribocorrosion behavior of Ti-13Zr-13Nb alloy remains limited, and studies on this alloy are relatively few. However, several recent studies have indicated that it represents a promising alternative for dental implant applications. Nevertheless, there is a clear lack of understanding about the durability of this alloy under the effect

of strong temperature shocks (5 °C and 60 °C). This study seeks to bridge this gap by monitoring bio-tribocorrosion mechanisms under these precise conditions for the first time, using the electrochemical noise (EN) approach.

The present study is novel in that:

Study of the bio-tribocorrosion behavior of Ti-13Zr-13Nb alloy at the low and high extremes of the oral environment temperature.

Use of EN characteristics for in-situ monitoring of passive film transitions and stability.

The aim of this work is to investigate the tribocorrosion behavior of a second-generation titanium alloy, Ti-13Zr-13Nb, intended for dental implant applications, under simulated oral conditions. The study focuses on evaluating the alloy response using EN measurements under open circuit potential OCP conditions, examining the effect of temperature as an oral environmental factor, and comparing its performance with a control condition representing the natural oral environment.

## 2. EXPERIMENTAL

Stander Ti–13Zr–13Nb with a diameter of 13 mm and a thickness of 3 mm was used in this investigation. Table 1 listed the chemical composition of alloy used; the specimen surfaces were prepared according to standard metallurgical preparation procedures to obtain smooth, homogeneous, and mirror-like surfaces suitable for tribocorrosion testing [13].

The tribocorrosion test was performed according to ASTM G133 using a ball-on-flat tribometer (UTS, Turkey) connected to a potentiostat/ galvanostat (Corr Test, China). EN technology was used during the tribocorrosion experiments under OCP to study the instantaneous electrochemical behavior resulting from the simultaneous interaction between wear and friction. This technique was adopted based on previous studies that demonstrated its effectiveness in monitoring transient changes in the behavior of inert metal surfaces, particularly the processes of partial surface layer removal and formation during sliding [14].

The lower part of the specimens was electrically connected to a potentiostat while isolated from the electrolyte solution, only the upper surface was exposed to the solution to serve as the working electrode (WE). The reference electrode (RE) was silver/silver chloride (Ag/AgCl), and a coiled platinum wire was used as the counter electrode (CE). The counter body was a 5 mm diameter, Grade 5 SiN ceramic sphere (Holis Shanghai Industrial Co., Ltd., China).

The test was performed under a vertical load of 1 N, with a cumulative sliding distance of 113 m, a stroke length of 10 mm, a sliding frequency of 1.57 Hz. During the tests, the voltage and current fluctuations spontaneously generated by the alloy surface during friction were recorded without the application of any external polarization, ensuring a realistic representation of the surface response under actual operating conditions. The recorded EN signals reflect the dynamic changes in the surface oxide layer during tribocorrosion under OCP conditions [15]. EN measurements were performed for each test throughout 4800 seconds. The sampling rate was 10 Hz (10 readings per second) to guarantee a high resolution and to catch the transitory events of the bio-tribocorrosion process. Pre-processing of the raw EN signals was done to eliminate any DC drift using polynomial detrending technique, and data analysis was performed with the OriginLab program. This procedure was necessary to make sure that the resulting noise characteristics, e.g., the noise resistance ($R_n$), really refer to the electrochemical stability of the Ti-13Zr-13Nb alloy without any effect on the trend of the signal.

Reference studies indicate that the thermal range in the oral cavity may vary from 0 °C to 70 °C, which may cause side effects on biological tissues [16]. However, due to the technical limitations of the equipment available in our laboratory, three temperatures were adopted for the present experimental work within the operable range, namely: 5 °C to represent low temperatures, 37 °C to represent normal body temperature, and 60 °C to represent the highest temperature available in the experiment, which approximates the temperatures of hot foods.

All tribocorrosion tests were repeated three times to assure statistical reliability. Results are reported as mean value ± standard deviation (SD). Results from all the situations studied were highly reproducible.

All tests were conducted in freshly prepared artificial saliva solutions with pH 6.8, the composition listed in Table 2.

**Table 1.** The chemical composition of alloy used in this investigation (wt.%)

| Sample | Microstructure | Ti | Zr | Nb | Other |
|---|---|---|---|---|---|
| Ti-13Zr-13Nb | β-rich | 62.65 | >16.19 | >19.72 | Balance |

**Table 2.** Chemical composition of artificial saliva [17]

| Chemical Compound | Chemical Formula | Weight (g) |
|---|---|---|
| Sodium Chloride | NaCl | 0.4 |
| Potassium Chloride | KCl | 0.4 |
| Calcium Chloride Dihydrate | $CaCl_2$. $2H_2O$ | 0.795 |
| Sodium Sulfide Nonahydrate | $Na_2S.9H_2O$ | 0.69 |
| Urea | $CH_4N_2O$ | 1 |
| Potassium Thiocyanate | KSCN | 0.3 |

The total volume loss was calculated using the following relationship:

$$V_t = A.L \quad (1)$$

where, ($V_t$) represents the total volume loss, (L) is sliding stroke length, with a value of 10 mm. The cross-sectional area of the wear track was calculated using the following equation:

$$A = \frac{R^2(\theta - \sin\theta)}{2} \quad (2)$$

where: (R) is the radius of the ball used in the tribocorrosion test (2.5 mm), (θ) is the angle of the circular segment forming

the wear track, which is calculated using:

$$\theta = 2\,sin^{-1}\left(\frac{a}{2R}\right) \quad (3)$$

(a) represents the wear track width.

To evaluate the contribution of mechanical and chemical factors to the overall degradation of the alloy, a mechanistic approach was adopted. The total material loss ($V_{total}$) was experimentally determined through dimensional measurements of the wear track using a profilometer. The chemical material loss ($V_{chem}$) was theoretically derived from the electrochemical current data generated during sliding, using Faraday's law:

$$v_{ch\,em} = \frac{MQ}{nF\rho} \quad (4)$$

where, (M) is the atomic weight, (n) is the valence number of the metal, (F) is Faraday's constant, (ρ) is the alloy density, Q the total charge generated during the friction process. Accordingly, the pure mechanical material loss ($V_{mech}$) was calculated as follows:

$$V_{mech} = Vtotal - Vchem \quad (5)$$

The wear track obtained in each specimen was evaluated using a scanning electron microscope (SEM).

## 3. RESULTS AND DISCUSSION

### 3.1 Tribocorrosion results using electrochemical noise technique

Figure 1 illustrates the change in potential over time for Ti-13Zr-13Nb alloy under three different temperatures. The figure demonstrates a clear sensitivity to temperature variation. In the pre-sliding stage, the alloy at 5 ℃ recorded the most noble (less negative) values, reflecting a reduction in the rate of electrochemical reactions and a noticeable relative stability of the passive oxide layer due to the reduced ionic activity of the solution, whereas the 37 ℃ specimen stabilized at intermediate values representing the standard behavior of the alloy under physiological conditions. At the onset of sliding, a sharp and sudden drop in potential toward active values occurred in all specimens, which is attributed to the mechanical destruction of the passive layer and the exposure of the metal surface to the solution, potentially creating local potential differences between the exposed areas in contact with the solution and the protected regions. It is also observed that the negative shift reached its highest value at 60 ℃ (approximately −0.33 V), while the 37 ℃ specimen maintained relative stability at a potential close to −0.26 V, compared with 5 °C (approximately −0.24 V). This variation indicates that increasing temperature slows the repassivation rate and increases the anodic dissolution rate under the effect of mechanical wear. The curve at 60 ℃ also shows high potential fluctuations, indicating a state of repeated dynamic interaction between mechanical removal and the repassivation process. Upon stopping the sliding, all specimens exhibited an immediate repassivation response, with faster recovery and a greater tendency toward noble values at the lower temperature. This indicates that the cooled medium enhances the stability of the protective oxide layer formed on the surface of the Ti-13Zr-13Nb alloy. This is consistent with study [16], which supports the finite element analysis (FEA) results published using ANSYS, showing a significant increase in thermal stress with rising temperature, where the highest von Mises stress values were recorded at 70 ℃. This increase in stress may contribute to destabilizing the passive layer on the surface of titanium alloys, explaining the larger fluctuations and the relative decrease in OCP values recorded in the present study at elevated temperatures.

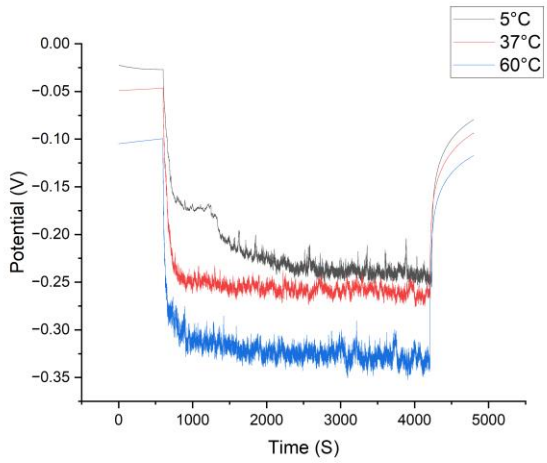


**Figure 1.** Potential as function of time for Ti-13Zr-13Nb alloy at three applied temperatures in artificial saliva

Figure 2 shows the EN current response of Ti-13Zr-13Nb alloy under three different temperatures. From the EN current density results, it is observed that the noise amplitude at 60 ℃ reached values approaching 100 μA/cm², which are high values indicating elevated localized electrochemical activity with increased corrosion concurrent with wear. The increase in temperature not only accelerated in kinetics, but also reduced the viscosity of the surrounding medium, thereby increasing the mass transport rate and the anodic reaction rate.

As for the behavior at 5 ℃, although it is chemically less active, the initial current spike indicates a different mechanical response of the passive oxide layer, as cooling often leads to a relative increase in oxide layer hardness, making it more susceptible to cracking under dynamic loading compared with its condition at body temperature (37 ℃). This explains why 37 ℃ recorded the lowest and most stable current, indicating that the Ti-13Zr-13Nb alloy exhibits the best biological and tribological performance under normal body temperature conditions and optimal stability.

The noticeable increase in electrochemical activity observed at 60 ℃ is consistent with the simulation results conducted in a previous study [16], which demonstrated that mechanical stresses (von Mises stress) reach their peak at elevated temperatures of 70 ℃, leading to weakening of oxide layer cohesion and accelerating its mechanical and chemical breakdown under sliding conditions.

Figure 3 shows the variation of the coefficient of friction (COF) with time for three Ti-13Zr-13Nb alloy specimens under the effect of three different temperatures. The COF behavior shows significant sensitivity to temperature variation, where body temperature (37 ℃) recorded the best (most stable) performance with values ranging between 0.28–0.40. This stability reflects a state of dynamic balance between removal

and the rate of repassivation, and also indicates surface stability during sliding, which reduces surface roughness during sliding and maintains the regularity of the wear track.

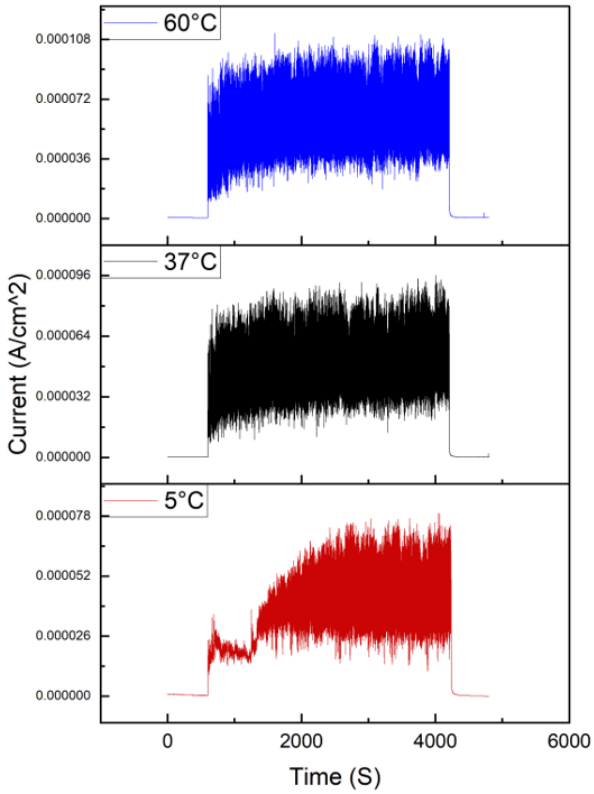


**Figure 2.** Current as a function of time for Ti–13Nb–13Zr alloy at three applied temperatures in artificial saliva

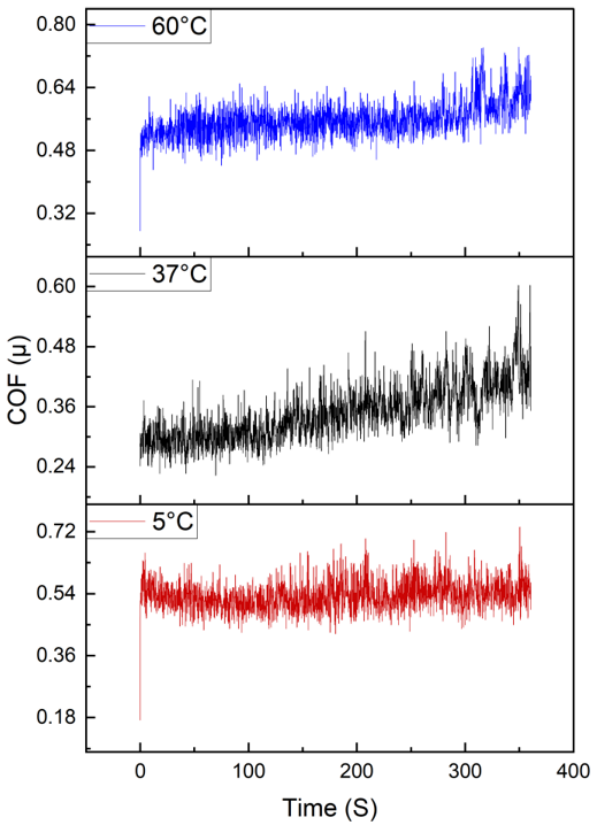


**Figure 3.** COF for Ti–13Nb–13Zr alloy at three applied temperatures in artificial saliva

In contrast, 60 °C recorded the highest friction values (0.55–0.70) with sharp fluctuations. This is attributed to the reduced stability of the oxide layer and the increased electrochemical activity leading to corrosion concurrent with wear (tribocorrosion), where the accumulated wear products act as abrasive particles that increase the mechanical resistance to sliding and raise the COF values.

At 5 °C, the increase in COF compared with 37 °C indicates that cooling alters the nature of the surface interaction, likely increasing resistance to plastic deformation and changing the properties of the medium in terms of viscosity, which hinders the motion of the counter-body and relatively increases friction forces. These results are consistent with the OCP and current density curves, as the relative instability of potential and current at extreme temperatures was directly reflected in the increase and instability of friction values.

For accurate comparison, the average COF was calculated for each temperature during the steady-state period. The results showed that the average value at 37 °C was the lowest at 0.35, while the average COF at 5 °C was 0.54, whereas the average increased significantly at 60 °C compared to the control specimen to reach 0.56, confirming the negative effect of high temperature on the tribological performance of the alloy.

These results are consistent with the study [18], which demonstrated that the stability of COF at body temperature (37 °C) is due to the dynamic balance between the rate of oxide layer removal and the repassivation rate. The study also supported that fluctuations in OCP values at elevated temperatures (60 °C) lead to increased wear products acting as abrasive particles, thereby significantly increasing COF under these conditions.

### 3.2 Surface characterization

The wear track obtained in each specimen was evaluated using a SEM, Figure 4 shows the SEM images of the wear track formed on the surface of the Ti-13Nb-13Zr alloy at three applied Temperatures. Figure 4(A) shows the SEM images of the wear track at 37 °C. It indicates clear agreement with the electrochemical results, as the track appears relatively uniform with limited surface roughness and absence of severe degradation. The presence of smooth and parallel longitudinal grooves indicates the predominance of abrasive wear as the main mechanism, with a complete absence of evidence of pitting corrosion, which explains the stability of COF at relatively low values. This surface morphological pattern reflects a stable balance between mechanical removal and repassivation, indicating that body temperature (37 °C) provides optimal conditions for the Ti-13Zr-13Nb alloy, where the protective oxide layer remains capable of protecting the surface from accelerated corrosion (synergistic effect) to compensate for damage caused by sliding, thereby limiting the effect of tribocorrosion under these conditions. Figure 4(B) indicates the wear track morphology characterized by parallel microscopic grooves extending along the sliding direction, indicating the predominance of abrasive wear. The absence of transverse cracks or delamination areas indicates good mechanical compatibility of the alloy at body temperature. This relatively polished surface appearance is consistent with the low and stable values of COF and current density, as these results indicate that the reconstruction of the passive oxide layer was sufficiently effective to counteract the mechanical damage resulting from sliding, thereby maintaining the

integrity of the implant interface through stabilization of the protective oxide layer during sliding. And Figure 4(C) shows the SEM images of the wear track at 60 ℃. Clear changes in wear severity are observed with increasing temperature to 60 ℃. The images show a clearly widened track with pronounced longitudinal grooves. This morphological change is consistent with the relatively unstable electrochemical behavior at this temperature, as the temperature increase accelerated anodic reactions within the wear region, making the passive layer less stable and more susceptible to mechanical removal during sliding. The high roughness observed in the images supports the relatively high COF values and is consistent with the wear mechanism at 60 ℃ being a combination of severe abrasion and accelerated chemical dissolution, i.e., a tribocorrosion mechanism, which may negatively affect the durability of the Ti-13Zr-13Nb dental implant alloy under such conditions. Figure 4(D) shows high-magnification morphology images of the 60 ℃ specimen. A clear morphological change is observed compared with the control specimen. The features were not limited to longitudinal grooves but also included the appearance of micro-pits and a clear accumulation of wear debris within the sliding track. The presence of these pits reflects the simultaneous interaction between mechanical effects and increased chemical activity due to heat, where the passive layer acquires a plastic and becomes thicker because of thermal activity. This morphological scene is consistent with the high fluctuations in the EN curves and the elevated COF values, as the accumulated debris acts as a protective cushion, increasing sliding resistance while shielding the metal from deep wear at these temperatures [19]. Figure 4(E) shows the SEM images of the wear surface of the specimen tested at 5 ℃. The images reveal a wear track characterized by clear abrasive grooves, but relatively narrower compared with the specimen tested at 60 ℃. The morphological behavior at this low temperature indicates that the oxide layer becomes more brittle and less ductile, leading to the appearance of fine surface cracks instead of the uniform plastic flow observed in the control specimen. These fine cracks contribute to explaining the increase in COF and the appearance of current pulses in the EN results, as each local crack in the layer momentarily exposes the metallic surface to the solution. Nevertheless, the reduced chemical activity at 5 ℃ limited the expansion of the wear region, making the surface damage less severe chemically and more concentrated on the mechanical abrasive aspect. Figure 4(F) shows the SEM images of the wear track morphology of the specimen tested at 5 ℃. It exhibited a distinct wear pattern clearly different from that of the specimen tested at 60 ℃. Despite the reduced chemical activity of the solution due to cooling, the surface showed signs of surface cracking and localized fragmentation of the passive layer.

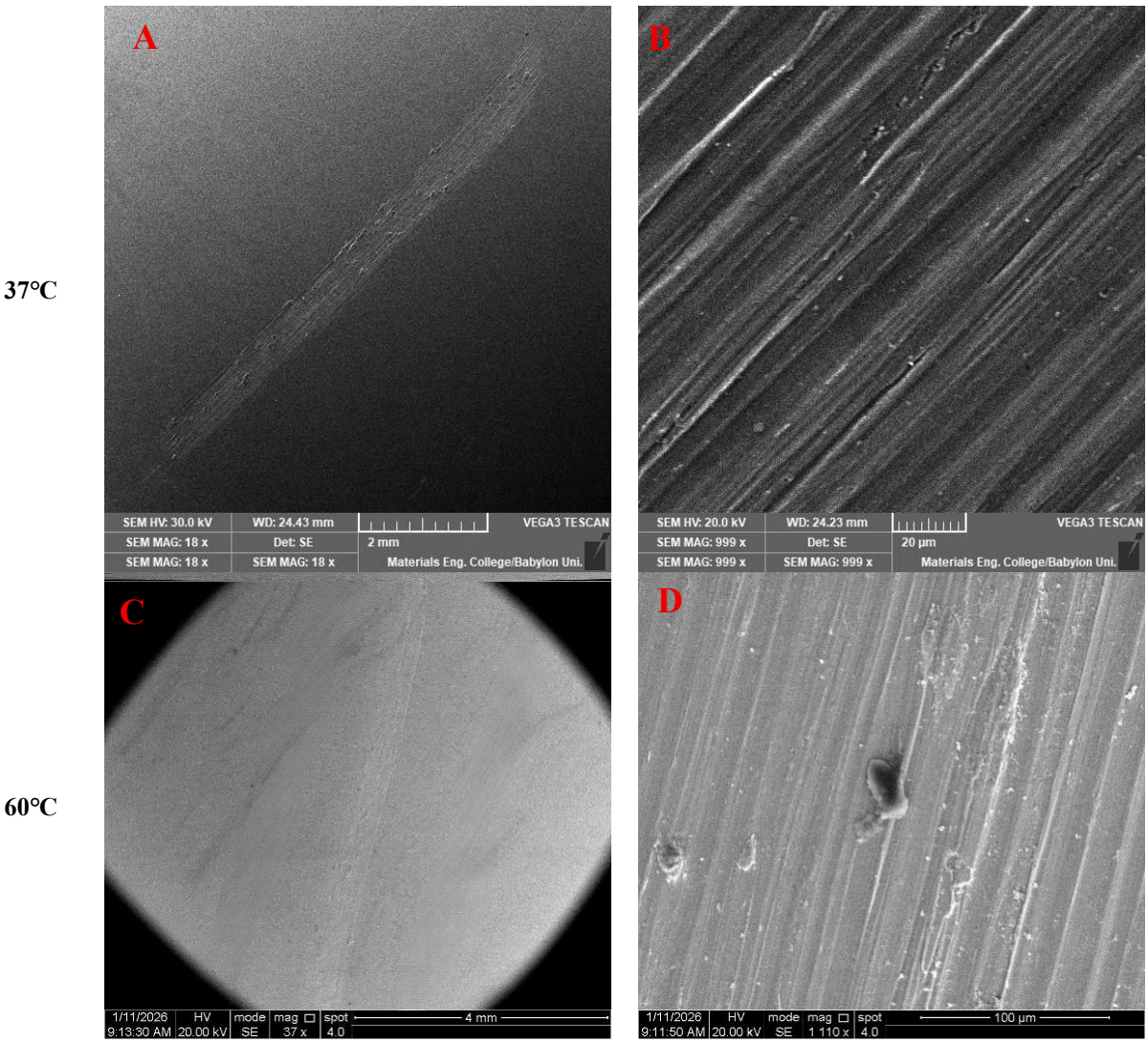

5°C

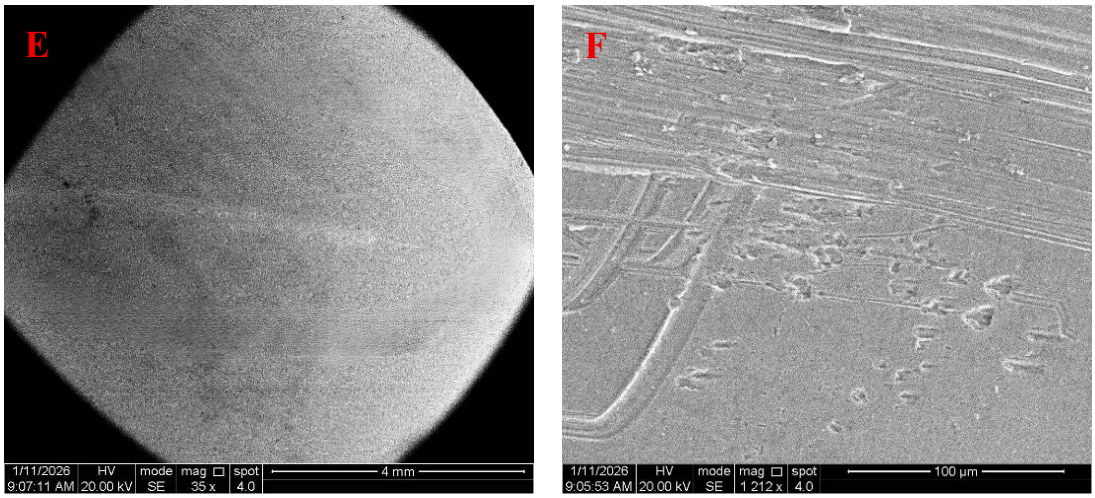


**Figure 4.** SEM surface morphology of the wear track Ti–13Nb–13Zr alloy at three applied temperatures in artificial saliva

### 3.3 The volume of material loss measurements

Table 3 and Figure 5 show the volumetric loss and wear rates, which show that temperature has a big and changing effect on the tribocorrosion of the Ti-13Zr-13Nb alloy. The sample tested at 5 °C had the highest total wear rate, which was 29.81% higher than the control sample tested at 37 °C. The big increase is because the mechanical mechanism ($V_{mech}$) is so common. At this low temperature the surface oxide layer undergoes a ductile-to-brittle transition and becomes more prone to micro-cracking and fragmentation. The SEM micrographs in Figures 4(E) and 4(F) with deep abrasive grooves and clear surface micro-cracks validate this embrittlement morphologically. This gentle reaction allows for quick mechanical delamination of the protective $TiO_2$ coating, which exactly correlates with the peak in ($V_{mech}$) loss seen in the quantitative data [20]. On the other hand, raising the temperature to 60 °C caused a big drop in the total amount of material lost, with a change rate of -71.00% compared to normal conditions. Instead, a large reduction in mechanical loss was found owing to the large chemical contribution from the thermal activation of anodic breakdown. This occurrence is linked to the creation of a thick viscous oxide layer that acts as a "protective cushion" as shown in Figures 4(C) and 4(D) in the SEM image. This layer, produced by enhanced chemical activity, shields the metal substrate from direct mechanical friction. Therefore, the thermal activation at 60 °C supports a protective system in which the stability and the elasticity of the inert layer are higher than the mechanical shear forces, leading to a minimum overall volume loss.

Figure 5 illustrates the graphical representation of the total volume loss and its mechanical and chemical components at different temperatures. The figure clearly shows the effect of temperature on the contribution of each mechanism to volume loss, where the chemical loss contribution increases at high temperature, while the mechanical contribution is relatively lower.

**Table 3.** Tribocorrosion results for Ti–13Nb–13Zr alloy at three applied temperatures in artificial saliva

| Temperatures Value (°C) | $V_{Total}$ ($mm^3$) | $V_{Chem}$ ($mm^3$) | $V_{Mech}$ ($mm^3$) | $V_{chem}/V_{total}$ | Wear Depth (µm) | Wear Rate (K) ($mm^3/N.m$) | Percentage Change % |
|---|---|---|---|---|---|---|---|
| 5 | $8.125 \times 10^{-2}$ ±0.015 | $2.32 \times 10^{-3}$ ± 0.008 | $7.89 \times 10^{-2}$ ± 0.012 | $2.86 \times 10^{-2}$ ± 0.002 | 18 ± 1 | $2.68 \times 10^{-4}$ ± 0.05 | 29.81% |
| Control (37) | $6.259 \times 10^{-2}$ ± 0.011 | $3.01 \times 10^{-3}$ ± 0.009 | $5.96 \times 10^{-2}$ ± 0.010 | $4.81 \times 10^{-2}$ ± 0.003 | 73 ± 3 | $9.23 \times 10^{-4}$ ± 0.08 | --- |
| 60 | $1.815 \times 10^{-2}$ ± 0.005 | $1.71 \times 10^{-3}$ ± 0.005 | $1.64 \times 10^{-2}$ ± 0.004 | $9.41 \times 10^{-2}$ ± 0.006 | 12 ± 1 | $1.25 \times 10^{-3}$ ± 0.12 | -71.00% |

Note: Data are presented as mean (±) standard deviation for (n =3) independent measurements.

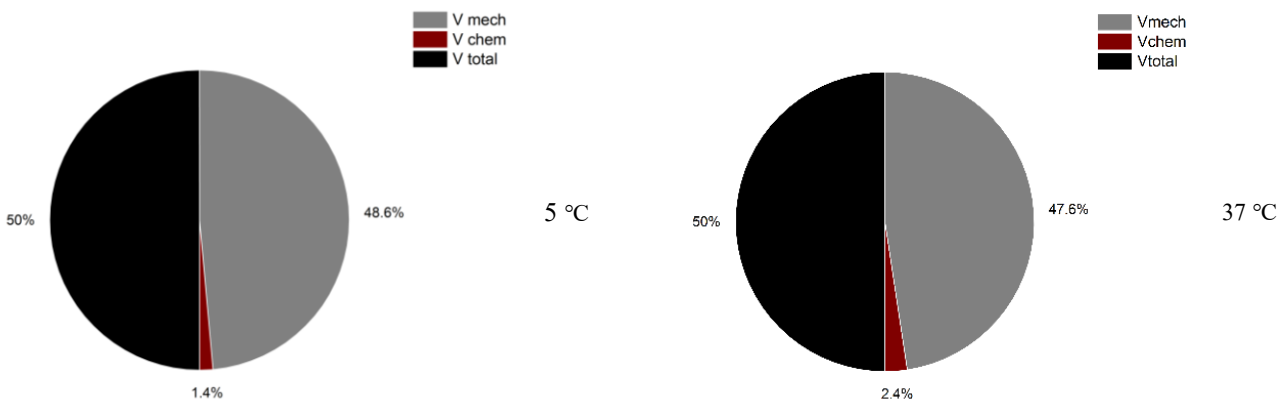

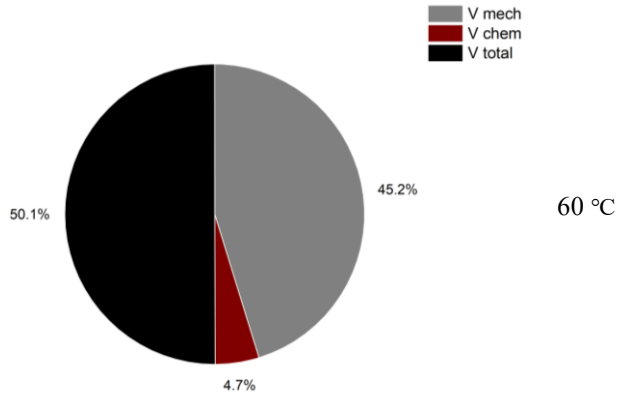


**Figure 5.** Vt, $V_{chem}$ and $V_{mech}$ for Ti–13Nb–13Zr alloy at three applied temperatures in artificial saliva

## 4. CONCLUSIONS

The main conclusions of this investigation can be summarized as follows:

1. Temperature showed a direct and clear effect on the tribocorrosion behavior of the Ti–13Zr–13Nb alloy in terms of passive layer stability, the distribution of mechanical and chemical loss, as well as changes in wear track morphology.

2. The open-circuit potential went down the greatest, the current density noise was the loudest, and the friction coefficient was the highest when the temperature was high (60 °C). This means that wear and corrosion occurred faster and had a stronger effect when they happened at the same time.

3. The best balance between mechanical removal and repassivization was found at body temperature (37 °C). This led to the lowest and most stable coefficient of friction, more consistent electrochemical behavior, and modest volume loss compared to other temperatures.

4. Electrochemical activity went down a lot when the temperature was low (5 °C). But the whole loss process was about how the oxide layer changed physically at high temperatures, making it more brittle and changing its mechanical characteristics.

5. The volume loss data showed that lower temperatures produced higher material loss overall because they made the mechanical contribution bigger. On the other hand, higher temperatures generated the least amount of loss overall since they made chemicals work better.

6. The results reveal that the alloy works best at physiological conditions (37 °C), when there is a stable dynamic equilibrium between the mechanical and chemical parts. Changes in temperature that make it hotter or colder throw off this equilibrium and make synergistic corrosion worse.

## REFERENCES

[1] Li, Y., Yang, C., Zhao, H., Qu, S., Li, X., Li, Y. (2014). New developments of ti-based alloys for biomedical applications. Materials, 7(3): 1709-1800. https://doi.org/10.3390/ma7031709

[2] Lambjerg-Hansen, H., Asmussen, E. (1997). Mechanical properties of endodontic posts. Journal of Oral Rehabilitation, 24(12): 882-887. https://doi.org/10.1111/j.1365-2842.1997.tb00289.x

[3] Oliveira, V., Chaves, R., Bertazzoli, R., Caram, R. (1998). Preparation and characterization of TI-AL-NB alloys for orthopedic implants. Brazilian Journal of Chemical Engineering, 15(4): 326-333. https://doi.org/10.1590/s0104-66321998000400002

[4] Hussein, M.A., Mohammed, A.S., Al-Aqeeli, N. (2015). Wear characteristics of metallic biomaterials: A review. Materials, 8(5): 2749-2768. https://doi.org/10.3390/ma8052749

[5] More, N., Diomidis, N., Paul, S., Roy, M., Mischler, S. (2011). Tribocorrosion behavior of β titanium alloys in physiological solutions containing synovial components. Materials Science and Engineering: C, 31(2): 400-408. https://doi.org/10.1016/j.msec.2010.10.021

[6] Geetha, M., Singh, A.K., Asokamani, R., Gogia, A.K. (2009). Ti based biomaterials, the ultimate choice for orthopaedic implants – A review. Progress in Materials Science, 54(3): 397-425. https://doi.org/10.1016/j.pmatsci.2008.06.004

[7] Khulief, Z.T., H., M.A. (2022). Corrosion behavior of different types titanium alloys for biomedical applications. AIP Conference Proceedings, 2450: 020023. https://doi.org/10.1063/5.0095387

[8] Khulief, Z. (2018). Tribological, electrochemical, and tribocorrosion behaviour of new titanium biomedical alloys. Doctoral dissertation. University of Sheffield.

[9] Pu, J., Liu, C., Si, Y., Cui, W., Zhang, C., Song, J. (2026). Tribocorrosion of metallic biomaterials under simulated inflammation conditions: Current status and future prospects. Advanced Healthcare Materials, 15(7): e02419. https://doi.org/10.1002/adhm.202502419

[10] Ponthiaux, P., Wenger, F., Drees, D., Celis, J. (2004). Electrochemical techniques for studying tribocorrosion processes. Wear, 256(5): 459-468. https://doi.org/10.1016/s0043-1648(03)00556-8

[11] Mischler, S. (2008). Triboelectrochemical techniques and interpretation methods in tribocorrosion: A comparative evaluation. Tribology International, 41(7): 573-583. https://doi.org/10.1016/j.triboint.2007.11.003

[12] Zirari, T., Trabadelo, V. (2024). A review on wear, corrosion, and wear-corrosion synergy of high entropy alloys. Heliyon, 10(4): e25867. https://doi.org/10.1016/j.heliyon.2024.e25867

[13] Neville, A., Hodgkiess, T. (1999). Characterisation of high-grade alloy behaviour in severe erosion–corrosion conditions. Wear, 233-235: 596-607. https://doi.org/10.1016/s0043-1648(99)00220-3

[14] Namus, R.M., Al-Rubaye, A.D.G., Alali, M.S. (2025).

Using electrochemical noise EN to study the tribocorrosion mechanisms for Ti6Al4V and SS 304 in ringer's solution. Journal of Bio- and Tribo-Corrosion, 12: 24. https://doi.org/10.1007/s40735-025-01092-8

[15] A Naumova, E., Kuehnl, P., Hertenstein, P., Markovic, L., A Jordan, R., Gaengler, P., Arnold, W.H. (2012). Fluoride bioavailability in saliva and plaque. BMC Oral Health, 12: 3. https://doi.org/10.1186/1472-6831-12-3

[16] Kriswanto, K., Jamari, J., Bayuseno, A.P., Setiawan, F., Fitriyana, D.F., Huda, K., Widodo, R.D., Dhiaulhaque, D., Al Afkar, N.B. (2025). Stress and displacement simulation of the posterior dental implants on variations of applied materials and temperatures. Journal of Advanced Research in Applied Mechanics, 135(1): 164-179. https://doi.org/10.37934/aram.135.1.164179

[17] Fangaia, S.I.G., Messias, A., Guerra, F.A.D.R.A., Ribeiro, A.C.F., Valente, A.J.M., Nicolau, P.M.G. (2024). Evaluation of the tribocorrosion behavior of Ti-6Al-4V biomedical alloy in simulated oral environments. Processes, 12(7): 1283. https://doi.org/10.3390/pr12071283

[18] Cruz, H.V., Souza, J.C.M., Henriques, M., Rocha, L.A., Cruz, H.V., Souza, J.C.M., Rocha, L.A. (2011). Tribocorrosion and bio-tribocorrosion in the oral environment: The case of dental implants. Biomedical Tribology, 1(1): 1-33.

[19] Reed, B., Wang, R., Lu, R. Y., Qu, J. (2021). Autoclave grid-to-rod fretting wear evaluation of a candidate cladding coating for accident-tolerant fuel. Wear, 466-467: 203578. https://doi.org/10.1016/j.wear.2020.203578

[20] Neto, M.Q., Rainforth, W.M. (2021). Effect of potential and microstructure on the tribocorrosion behaviour of beta and near beta Ti alloys II. Journal of Bio- and Tribo-Corrosion, 7(4): 1-12. https://doi.org/10.1007/s40735-021-00578-5